Assessment of transferrin recycling by Triplet Lifetime Imaging in living cells

Matthias Geissbuehler,[1,*] **Zuzana Kadlecova,**[2] **Harm-Anton Klok,**[2] **and Theo Lasser**[1]

[1] *Laboratoire d'Optique Biomédicale LOB, Ecole Polytechnique Fédérale de Lausanne (EPFL), Station 17, CH-1015 Lausanne, Switzerland*

[2] *École Polytechnique Fédérale de Lausanne (EPFL), Institut des Matériaux and Institut des Sciences et Ingénierie Chimiques, Laboratoire des Polymères, Bâtiment MXD, Station 12, CH-1015 Lausanne, Switzerland*

[*] *matthias.geissbuehler@a3.epfl.ch*

Abstract: An optical method is presented that allows the measurement of the triplet lifetime of a fluorescent molecule. This is a characteristic specific to each fluorophore. Based on differences in triplet lifetimes of two fluorescent species (autofluorescence versus label), this novel approach measures relative quantities of a transmembrane receptor and associated fluorescently labeled ligand during its recycling in living cells. Similarly to fluorescence-lifetime based methods, our approach is almost insensitive to photobleaching. A simple theory for unmixing two known triplet lifetimes is presented along with validation of the method by measurements of transferrin recycling in a model system based on chinese hamster ovarian cells (CHO). Transferrin is the delivery carrier for Fe^{3+} to the cell.

OCIS codes: (180.2520) Fluorescence microscopy; (170.3650) Lifetime-based sensing; (100.2960) Image analysis; (170.2655) Functional monitoring and imaging; (170.3880) Medical and biological imaging; (170.1420) Biology; (170.0180) Microscopy

References and links

1. M. Geissbuehler, T. Spielmann, A. Formey, I. Märki, M. Leutenegger, B. Hinz, K. Johnsson, D. Van De Ville, and T. Lasser, "Triplet imaging of Oxygen consumption during the contraction of a single smooth muscle cell (A7r5)," Biophys J **98**, 339–349 (2010).
2. T. Sandén, G. Persson, P. Thyberg, H. Blom, and J. Widengren, "Monitoring kinetics of highly environment sensitive states of fluorescent molecules by modulated excitation and time-averaged fluorescence intensity recording," Anal Chem **79**, 3330–3341 (2007).
3. W. Rumsey, J. Vanderkooi, and D. Wilson, "Imaging of phosphorescence: A novel method for measuring oxygen distribution in perfused tissue," Science **241**, 1649–1651 (1988).
4. J. Vanderkooi, G. Maniara, T. Green, and D. Wilson, "An optical method for measurement of dioxygen concentration based upon quenching of phosphorescence," J Biol Chem **262**, 5476–5482 (1987).
5. G. Baravalle, D. Schober, M. Huber, N. Bayer, R. Murphy, and R. Fuchs, "Transferrin recycling and dextran transport to lysosomes is differentially affected by bafilomycin, nocodazole, and low temperature," Cell Tissue Res **320**, 99–113 (2005).
6. H. Li and Z. M. Qian, "Transferrin/transferrin receptor-mediated drug delivery," Med Res Rev **22**, 225–250 (2002).
7. B. Alberts, *Molecular biology of the cell* (Garland Science - Taylor&Francis group, 2008).
8. D. Sheff, L. Pelletier, C. O'Connell, G. Warren, and I. Mellman, "Transferrin receptor recycling in the absence of perinuclear recycling endosomes," J Cell Biol **156**, 797–804 (2002).
9. Y. J. Yu, Y. Zhang, M. Kenrick, K. Hoyte, W. Luk, Y. Lu, J. Atwal, J. M. Elliott, S. Prabhu, R. J. Watts, and M. S. Dennis, "Boosting brain uptake of a therapeutic antibody by reducing its affinity for a transcytosis target," Sci Transl Med **3**, (2011).

10. P. Friden, L. Walus, G. Musso, M. Taylor, B. Malfroy, and R. Starzyk, "Anti-transferrin receptor antibody and antibody-drug conjugates cross the blood-brain barrier," P Natl Acad Sci USA **88**, 4771–4775 (1991).
11. E. Daro, P. Van Der Sluijs, T. Galli, and I. Mellman, "Rab4 and cellubrevin define different early endosome populations on the pathway of transferrin receptor recycling," P Natl Acad Sci USA **93**, 9559–9564 (1996).
12. J. Gruenberg and F. Maxfield, "Membrane transport in the endocytic pathway," Curr Opin Cell Biol **7**, 552–563 (1995).
13. R. Ghosh, D. Gelman, and F. Maxfield, "Quantification of low density lipoprotein and transferrin endocytic sorting in HEp2 cells using confocal microscopy," J Cell Sci **107**, 2177–2189 (1994).
14. D. M. Sipe and R. F. Murphy, "High-resolution kinetics of transferrin acidification in BALB/c 3T3 cells: exposure to pH 6 followed by temperature-sensitive alkalinization during recycling," P Natl Acad Sci USA **84**, 7119–7123 (1987).
15. T. McGraw and F. Maxfield, "Human transferrin receptor internalization is partially dependent upon an aromatic amino acid on the cytoplasmic domain," Cell regul **1**, 369–377 (1990).
16. J. R Lakowicz, *Principles of Fluorescence Spectroscopy* (Springer, 2006).
17. F. Maxfield and T. McGraw, "Endocytic recycling," Nat Rev Mol Cell Biol **5**, 121–132 (2004).
18. B. Grant and J. Donaldson, "Pathways and mechanisms of endocytic recycling," Nat Rev Mol Cell Biol **10**, 597–608 (2009).
19. A. Durrbach, D. Louvard, and E. Coudrier, "Actin filaments facilitate two steps of endocytosis," J Cell Sci **109**, 457–465 (1996).
20. N. Muller, P. Girard, D. Hacker, M. Jordan, and F. Wurm, "Orbital shaker technology for the cultivation of mammalian cells in suspension," Biotechnol Bioeng **89**, 400–406 (2005).

1. Introduction

Triplet lifetime imaging allows the lifetime of the triplet state of fluorescent molecules to be measured [1, 2]. In contrast to methods assessing the triplet lifetime directly with the help of the phosphorescence emission of special phosphorescent-dyes [3, 4], triplet lifetime imaging is based on the fluorescence emission. This results in a much stronger signal compared to phosphorescence emission and so to an enhanced sensitivity of the method allowing for fundamentally better spatial and temporal resolution [1].

In this work, we employ triplet lifetime imaging to assess the recycling pathway of transferrin and its receptor which serves as a model transmembrane protein. Transferrin, is a serum glycoprotein with two binding sites for Fe^{3+} ions. The protein binds to a specific transferrin receptor (TfnR) on the plasma-membrane and is internalized upon binding to the ligand via clathrin-mediated endocytosis [5, 6]. The endosomal environment causes the release of the iron from the transferrin [5, 7]. The iron-free transferrin (apotransferrin) is then recycled back to the plasma-membrane together with the receptor where they dissociate to release the transferrin to the outside of the cell from where the cycle can be re-initiated [5, 8].

The strong scientific interest in transferrin and the potential application in medicine and biology stems from its successful use as a general delivery vector. Its iron binding site can bind other metal ions for therapeutic or diagnostic use. In addition by conjugating transferrin to small molecular drugs or protein sequences of interest, it can be employed as a general delivery system [6]. Moreover, the receptor-mediated transcytosis pathway was identified as a potential way to transport therapeutics across the blood-brain barrier [9, 10]. In this context transferrin guided drug delivery is under intense investigation. And finally, thanks to a multitude of studies, its internalization and trafficking properties are well known and thus provide an optimal validation system for this study.

Two different transferrin recycling pathways have been identified: a fast recycling directly from early endosomes and a slow recycling via the perinuclear recycling compartment (PNRC) [11–13]. Figure 1 shows an overview of the uptake and recycling pathways.

The assessment of the receptor and ligand quantities and mechanistic studies of their recycling pathways are mainly done by the usage of ensemble-based techniques where entire cell-populations are considered. For example by flow cytometry [14] or by using radiolabels [8, 15]. Alternatively, fluorescence microscopy based techniques have been employed to describe the

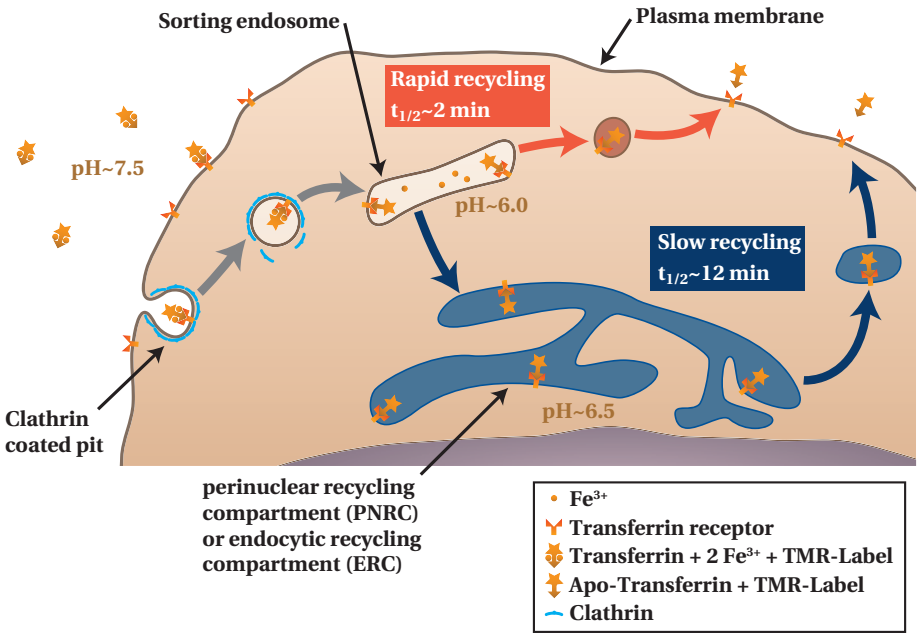

Fig. 1. Transferrin uptake and recycling pathways as described in various publications [5, 8, 12, 13, 17–19]. The pH and typical half-lifetimes are indicative values adopted from [17].

sub-cellular stages of the recycling pathway. In this case the relative receptor quantities are generally *inferred* from the detected fluorescence intensity [11–13]. However this is prone to errors, due to fluorophore bleaching and photophysical effects caused by the microenvironment of the observed label [16].

We propose to assess the transferrin recycling pathway on a sub-cellular level by using triplet lifetime imaging. Our results show that the approach described ensures accurate assessment of the relative quantities of transmembrane proteins during the dynamic recycling-process. The main advantage of this method in comparison to standard techniques is the fast acquisition rate, allowing very early stages of the recycling pathways to be visualized. Our approach is nearly insensitive to bleaching because it is based on the lifetime of the triplet state and can be performed easily on living cells. It improves the measurement sensitivity especially in the low transferrin quantity regime. Our results are based on differences in triplet lifetimes between the autofluorescence (background) and the TMR-labeled transferrin. Finally, these results support the usefulness of triplet lifetime imaging technique for investigating cell functions.

2. Materials and methods

2.1. Cell cultivation

Suspension cell culture of CHO DG44 cells were maintained in square-shaped glass bottles (250 mL) in serum free ProCHO5 cell culture medium (Lonza AG, Verviers, Belgium) supplemented with 13.6 mg L^{-1} hypoxanthine, 3.84 mg L^{-1} thymidine and 4 mM glutamine (SAFC Biosciences, St. Louis, MO) as described by Muller et al. [20]. 24h prior to the experiment CHO cells were plated in complete ProCHO5 medium supplemented with 10% fetal calf serum. Cells were seeded on micro-dishes (μ-Dish, Ibidi, Martinsfried, Germany). Prior to the experiment, the cells were washed twice with either RPMI or HBSS and incubated for 5 min at 37°C in

the respective media [5]. In order to eliminate the effect of buffer composition RPMI or HBSS were compared. Experiments carried out in both media lead to identical measurement results. The washing step was followed by a 20 min incubation in serum-free DMEM-medium at 37°C followed by repeated washing steps and incubation in serum-free medium. The cells were then incubated for 7 min at 37°C with tetramethylrhodamine (TMR) labeled transferrin obtained from human serum (T-2872, Invitrogen, Basel, Switzerland) at a concentration of 500 µg/ml, followed by three washing steps with complete ProCHO5, which was employed for the imaging. Dishes were placed on 37°C heating stage mounted on the wide field microscope and maintained at 5% CO2 atmosphere.

2.2. *Molecular fluorescence upon modulated excitation*

The behaviour of fluorophores upon excitation by light, can be described by a three state level Jablonski diagram with a singlet ground state, a singlet excited state and a triplet excited state (Fig. 2(a)). The triplet state has typically a lifetime that is three to four magnitudes longer (microseconds) than the lifetime of the excited singlet state (nanoseconds).

The three state Jablonski diagram is governed by the following rate equations

$$\frac{\mathrm{d}}{\mathrm{d}t}\begin{bmatrix} P_0 \\ P_1 \\ P_T \end{bmatrix} = \begin{bmatrix} \frac{P_1}{\tau_S} + \frac{P_T}{\tau_T} - \frac{P_0}{\tau_{ex}} \\ -\frac{P_1}{\tau_S} - \frac{P_1}{\tau_{isc}} + \frac{P_0}{\tau_{ex}} \\ \frac{P_1}{\tau_{isc}} - \frac{P_T}{\tau_T} \end{bmatrix} \tag{1}$$

where P_0, P_1 and P_T are the respective populations of the singlet states and the triplet state, τ_S is the lifetime for the singlet state relaxation, τ_{isc} is the intersystem crossing lifetime from the excited singlet state to the triplet state, τ_T is the triplet state lifetime and τ_{ex} is the excitation lifetime, which is a measure for the incoming intensity taking into account the absorption cross section of the molecule (τ_{ex} is often also denoted as α^{-1} where α is the excitation rate).

Triplet lifetime imaging employs a modulated excitation scheme. By varying the pulse length of illumination pulses, the triplet state population of the fluorophores can be tuned. Illumination with long pulses achieves a steady triplet state population, while short pulses only populate the triplet state to a limited amount. This results in a modification of the proportional amount of emitted photons: if only few molecules are ”pushed” onto the non-radiative triplet state, the fluorescence emission is comparably stronger. Figure 2(b) shows a simulation of the emitted fluorescence intensity upon illumination with a modulated excitation scheme that keeps an isodosis of light illumination.

As has been shown [1] the triplet state population at equilibrium is given by

$$P_T^{\mathrm{eq}} = \frac{\Phi_T \tau_T}{\tau_{ex} + \tau_S + \Phi_T \tau_T} \tag{2}$$

Where Φ_T describes the triplet quantum yield

$$\Phi_T = \frac{k_{isc}}{k_{rad.} + k_{non\text{-}rad.} + k_{isc}} \approx \frac{\tau_S}{\tau_{isc}}. \tag{3}$$

2.3. *Triplet lifetime unmixing*

Our results are based on differences in triplet lifetimes of two fluorescent species ($\tau_{T,\,autofluorescence} = 5.5\mu s$ for the autofluorescence vs $\tau_{T,\,dye} = 2.5\mu s$ for the TMR-label). In order to assess the relative quantity of each, an expression has to be found that allows *unmixing* of the measured triplet lifetimes based on the known triplet lifetimes of each species.

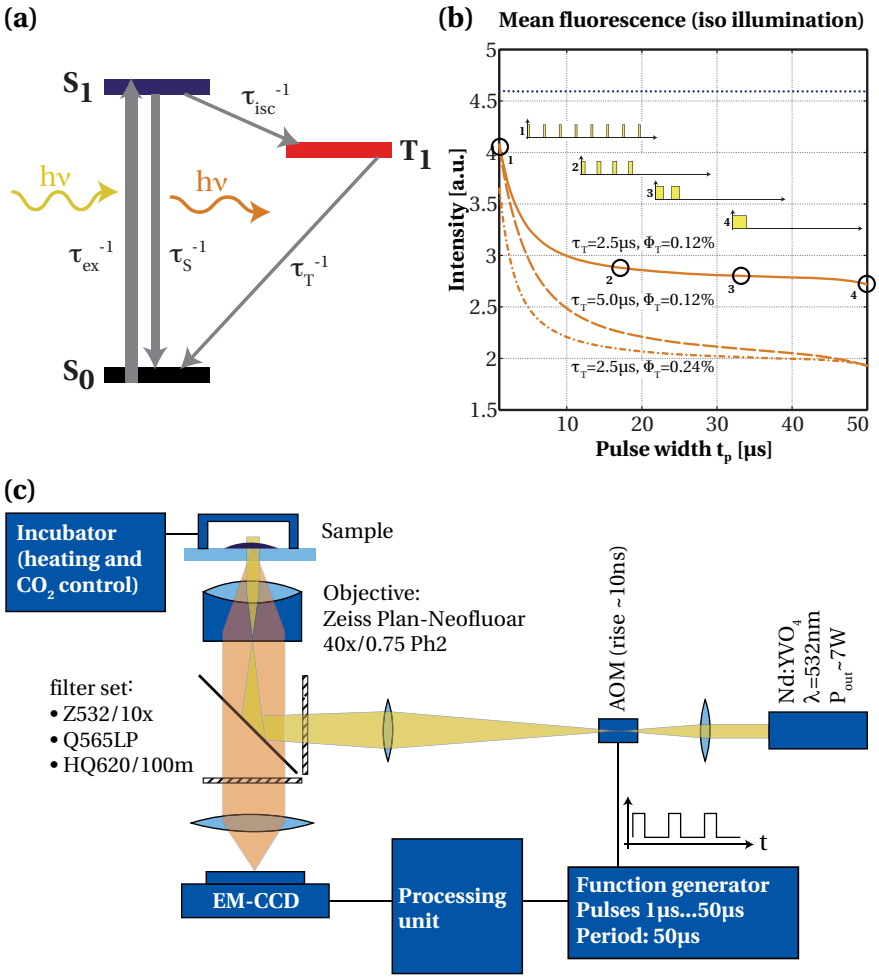

Fig. 2. (a) Jablonski diagram of a fluorescent molecule with three states. (b) Simulation of fluorescence emission when using a pulsed excitation with an iso-dosis of light illumination. Three different cases of τ_T and Φ_T are shown. For all curves $\tau_s = 2.3$ ns, and $\tau_{ex} = 2.1$ ns (corresponding to an illumination intensity of 10 mW/µm^2 for TMR) and pulse widths vary from 1 to 50 µs with a repetition rate of 50 µs. (c) Schematic drawing of the triplet lifetime imaging setup. Beamshaping ensured a spot radius of ≈175 µm at the sample plane, resulting in a maximum intensity of ≈0.6 mW/µm^2. The cell-incubator maintained optimal temperature (37°C), humidity and carbon dioxide content of the atmosphere in the observation chamber (CO_2 at 5%).

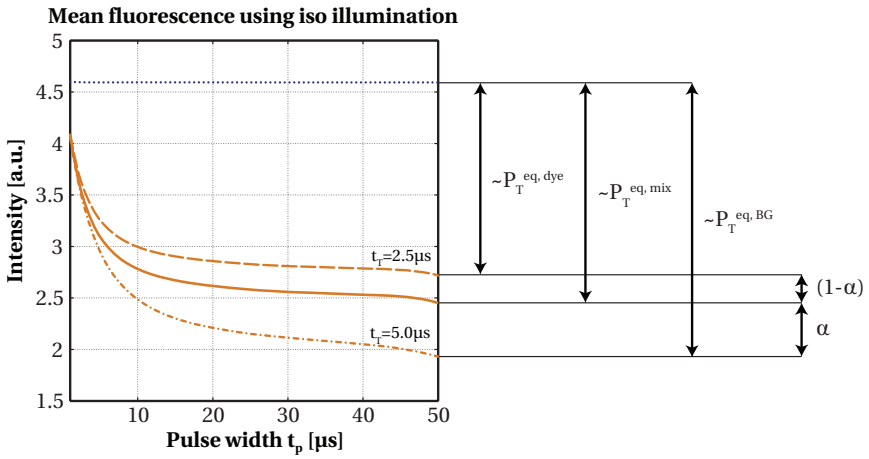

Fig. 3. Unmixing of two known triplet lifetimes with the help of the triplet population for a constant excitation at equilibrium P_T^{eq}.

Unfortunately, the expression describing the fluorescence intensity as a function of the pulse width under iso-dosis illumination (Eq. 4 in reference [1]) is too complex to yield an analytical solution to the unmixing-problem. As a simple but powerful alternative, we propose to start from the expression for the relative triplet population (eq. 2) and describe the mixing simply with the help of this expression. Figure 3 shows an overview of the idea. Hence we find

$$\begin{aligned} P_T^{\text{eq, mix}} &= \alpha P_T^{\text{eq, dye}} + (1-\alpha) P_T^{\text{eq, autofluorescence}} \\ \frac{\Phi_T \tau_{T,mix}}{(\tau_{ex}+\tau_S+\Phi_T\tau_{T,mix})} &= \frac{\alpha \Phi_T \tau_{T1}}{(\tau_{ex}+\tau_S+\Phi_T\tau_{T1})} + \frac{(1-\alpha)\Phi_T\tau_{T2}}{(\tau_{ex}+\tau_S+\Phi_T\tau_{T2})} \end{aligned} \tag{4}$$

This equation can easily be solved for α to reveal a simple analytical expression that describes the proportional amount of the dye (species 1) with respect to the autofluorescence (species 2) based on a mixture of the two species

$$\alpha = -\frac{(\tau_{T2}-\tau_{T,mix})(\tau_{ex}+\tau_S+\tau_{T1}\Phi_T)}{(\tau_{T1}-\tau_{T2})(\tau_{ex}+\tau_S+\tau_{T,mix}\Phi_T)} \tag{5}$$

The above equation determines the *proportional* amount, however, for an uptake assessment, we are also interested in the actual relative *quantity* and not just the relative proportion. The former is usually assessed with the help of the total fluorescence intensity within the cell. This is accepted generally as a quantitative measurement for the absolute amount of a fluorescence-labeled species [11–13], although it is rather error prone, by the fact that the intensity is sensitive to bleaching and photophysical effects (i.e. the microenvironment of the observed label influences the lifetime of the transient dark energy states). To overcome these limitations, we propose to limit the observation to a single shot per cell (to limit the photobleaching) and to extend the intensity based measure with the term we have just derived for the relative amount of the dye vs autofluorescence. As a result, we estimate that the uptaken relative quantity is proportional to

$$\begin{aligned} Q &\propto \left(1+\frac{I-I_{\text{BG}}}{I_{\text{BG}}}\right)\times\alpha \\ &\propto \frac{I}{I_{\text{BG}}}\times\alpha \end{aligned} \tag{6}$$

This result extends the sensitivity range for low quantities where the fluorescence intensity is close to the intensity of the background (autofluorescence) and leads to more reliable and stable results.

2.4. Triplet Lifetime Imaging

Figure 2(c) shows a schematic drawing of our setup. We have used a Millenia Pro 10s Nd:YVO4 laser ($\lambda = 532$ nm; Newport Spectra Physics) for our experiments. This laser provides up to 10 W of output power which is sufficient for the field size of our widefield setup. The beam was focused to a radius of ≈ 175 µm in the sample plane, resulting in a maximum intensity of ≈ 0.59 mW/µm^2. Fast modulation of the laser beam was achieved by an acousto-optical modulator (Gooch&Housego, AOM M200-4B/E-LD4 with driver A341 for a rise-time of ≈ 10 ns). The pulse sequence was generated with a function generator (Agilent, 33250A 80 Mhz). Splitting and filtering of excitation and emission signals was achieved by filters from Chroma (Z532/10x, Q565LP, HQ620/100m) and finally detected by a CCD-camera (Andor Luca EM-CCD). All devices were controlled with a Matlab application enabling convenient and rapid image acquisition and processing [1]. The samples have been imaged by eleven different pulse lengths (from 1 to 50 µs) with a periodicity of 50 µs, interlaced by three images at the shortest pulse length to estimate the bleaching. The total illumination dose was kept constant for each image with an illumination time of 0.1 ms.

Photo-bleaching is an important issue for our measurements and the intensity decrease due to photo-bleaching needs to be clearly separated from the intensity decrease due to the triplet lifetime photo kinetics. We estimate the bleaching during the measurement by an interlaced acquisition at the shortest pulse width. This allows a mono-exponential decay curve to be fitted to these interlaced images, which in turn yields parameters for the bleaching-correction of the acquisitions at different pulse widths [1]. Figure 4 shows an example of this image processing step.

The next processing step consists of fitting the triplet lifetime for each pixel. We fixed the singlet lifetime to $\tau_S = 2.4$ ns for the TMR-labeled Transferrin (as estimated by fluorescence lifetime measurements). Further on we employed $\Phi_T = 0.3\%$, which has been obtained by fitting triplet-lifetime and -yield over a larger region of interest (ROI) inside the measured CHO-cells. Fitting these two (non-linear) parameters by a standard optimization technique like the Marquardt-Levenberg algorithm is very slow and hence not suitable for processing an acquisition of 9 images containing 496x658 pixels. We circumvented this time consuming step and used an alternating least-squares approach for fast fitting. This resulted in typical fitting times of approximately 90 s for 152x115x9 pixels on a standard desktop computer (Intel Xeon 3.2 GHz, 2 GB RAM).

For improved measurement sensitivity, we performed an averaging of three sequentially recorded measurements. However we have found better fitting results for this work, when averaging the respective images *prior* to the fitting instead of averaging the fitting results as we did in the previous publication [1]. This different approach is motivated by the different time-scales of the two experiments: in our previous publication, we were interested in the oxygen consumption (≈ 10 s time-scale), while here we are interested in a slower recycling process ($\approx$ 1 min time-scale). Hence the expected changes in triplet lifetime are on a timescale that justify an averaging prior to the fitting.

In addition to these image processing steps, after calculation of the triplet lifetime image, we have selected manually regions of interest (ROI) around the cells. These ROI were used to calculate the mean triplet lifetime and standard deviation at a given time-point of the experiment. The mean is calculated with a fluorescence intensity weighting. The manual creation of regions of interest allowed the efficient rejection of cells that were no longer adhering to the cover slide

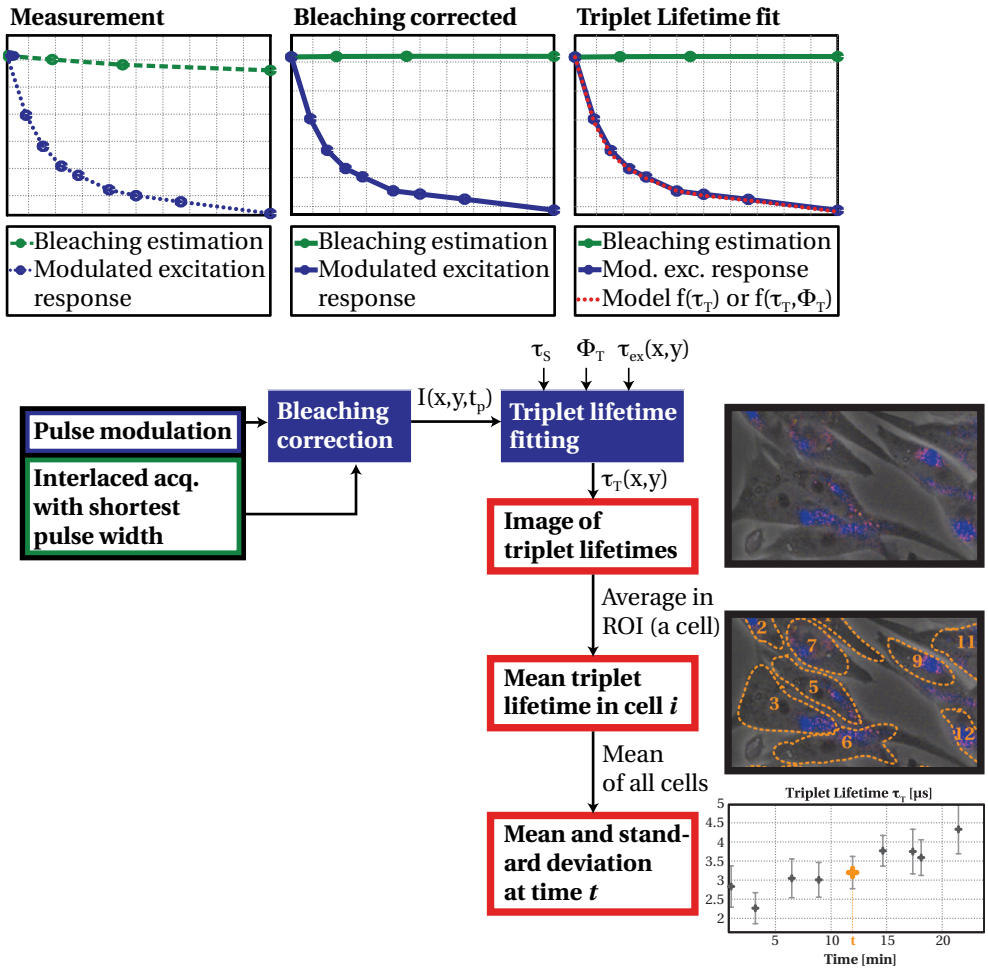

Fig. 4. Image processing steps. The triplet lifetime fitting is done pixel per pixel as discussed in our previous publication [1], involving knowledge of the singlet lifetime τ_S, the triplet yield Φ_T as well as the excitation rate τ_{ex}. The resulting triplet lifetime image is then averaged over small region of interests (ROI) corresponding to the respective cells in the image. This yields a mean and standard deviation for the triplet lifetime at the time-point t.

(most often dead cells) as well as artifacts of agglomerated labels.

3. Results

We have performed a series of experiments in living CHO cells to visualize and quantify transferrin recycling. Figure 5 shows a comparison of typical images for the three cases: (a) initial stage of the experiment of receptor mediated endocytosis (t=5 min), where the maximum quantity of labeled transferrin is contained within the cells, (b) later stage of the experiment (t=20 min), where the majority of fluorescently labeled transferrin is recycled, and (c) a typical image of the autofluorescence of CHO-cells excited at 532 nm. All the images have then been segmented manually in order to calculate the mean triplet lifetime over a single cell. Figure 6 shows a graph of the evolution of (a) the Triplet lifetime τ_T, and (b) the calculated TMR labeled transferrin fraction in %, where 100% corresponds to TMR and 0% to autofluorescence

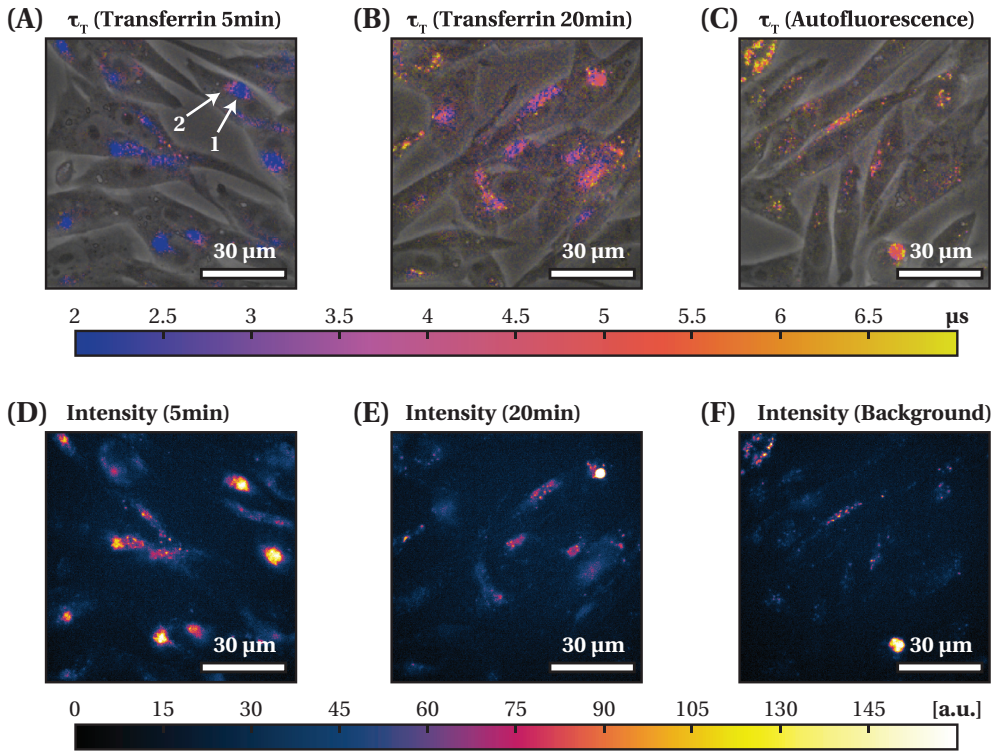

Fig. 5. Triplet lifetime images of transferrin recycling (color encoded). (a) Beginning of the experiment, where the cells are visualized after complete internalization of transferrin (t=5min). Some cells show two different areas: an area with short lifetime (1) and an area of longer lifetime (2). (b) An image of cells after 20 min, where a large amount of the internalized TMR labeled transferrin is recycled back into the medium and (c) a typical image of the autofluorescence of CHO-cells excited at 532 nm. The calculation employs a singlet lifetime of $\tau_S = 2.4$ ns for the TMR-labeled Transferrin (from fluorescence lifetime measurements) and $\Phi_T = 0.3\%$ (from triplet-lifetime and -yield fitting over ROI inside CHO-cells). (d-f) Corresponding fluorescence intensity images.

background. Further on (c) depicts the fluorescence intensity and finally (d) shows the relative quantity Q.

A measurement point corresponds to the intensity-weighted mean over approximately 10-20 cells. After every single observation, the field of observation has been moved to a new area on the dish in order to maintain minimal photobleaching to prevent erroneous intensity based measurement. The results show a large dispersion of measured values, due to the important variability of the quantity of the endocytosed transferrin.

4. Discussion and conclusion

We have successfully employed triplet lifetime imaging to assess the transferrin recycling in living cells. Our results prove that the method can provide an interesting extension to existing intensity based measures, since the lifetime is (almost) unaffected by photobleaching. The fluorescence intensity of the maximum endocytosed labeled transferrin is only about twice the intensity of the autofluorescence signal of CHO cells in these experimental conditions. As a result of the overall low transferrin associated fluorescence, intensity based assessment of the

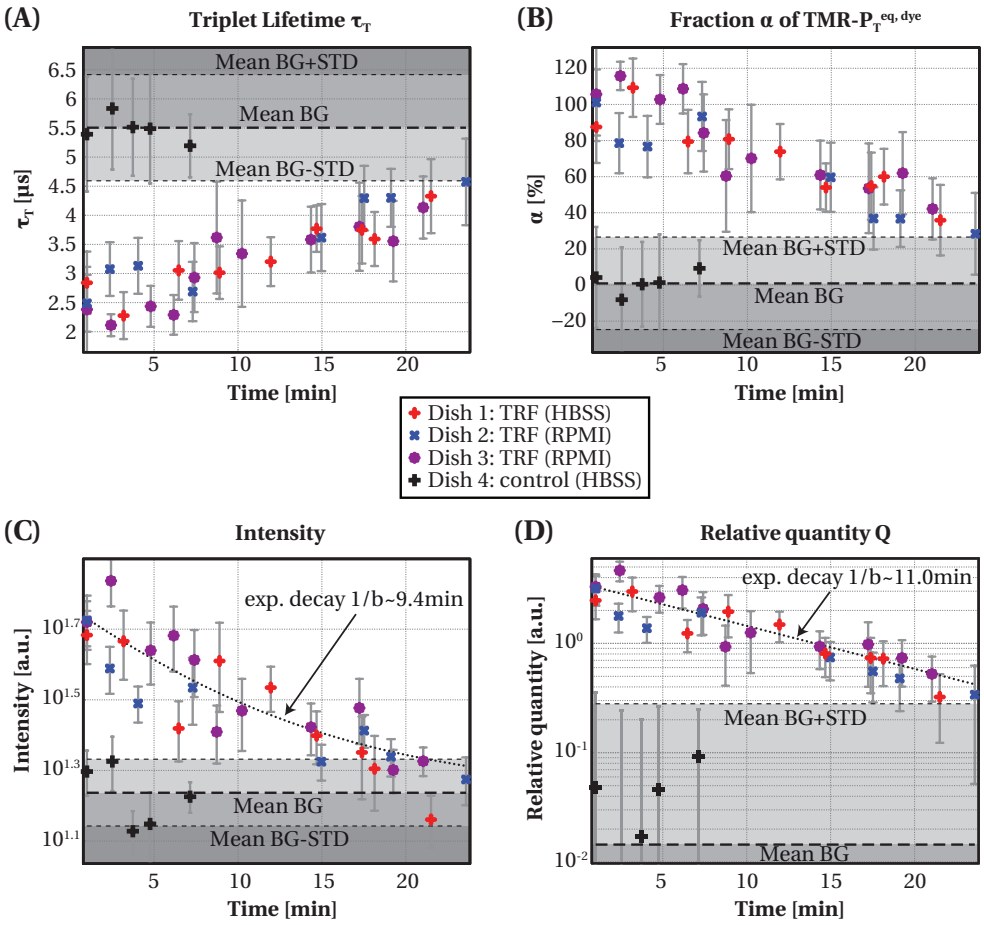

Fig. 6. Assessment of transferrin recycling in CHO-cells for three different experiments compared to the autofluorescence within these cells. (a) Triplet lifetime, (b) proportional amount of the dye (α=100%) compared to autofluorescence (α=0%) as defined by equation 5, (c) fluorescence intensity and (d) relative quantity of transferrin inside the cell Q as defined by equation 6. For the control measurement, we have repeated every washing and incubation step as for the experiments, except that we did not incubate the cells with transferrin-DMEM but only DMEM. For the relative quantity calculations, we used $\tau_{T,\,dye} = 2.5\mu s$ and $\tau_{T,\,autofluorescence} = 5.5\mu s$. Further on, the calculation employs a singlet lifetime of $\tau_S = 2.4$ ns for the TMR-labeled Transferrin (from fluorescence lifetime measurements) and $\Phi_T = 0.3\%$ (from triplet-lifetime and -yield fitting over ROI of an intracellular region of CHO-cells).

evolution of the recycling of transferrin can only be done up to twice the half-time of the recycling cycle (t $\approx$ 19 min). The lifetime dependent measure extends this range and allows the study of the transmembrane receptor associated with fluorescently labeled ligand on a longer time-scale.

In addition to these quantification experiments, our method also allows imaging during the recycling of the transmembrane protein. The triplet lifetime provides an additional channel of information to the fluorescence intensity image which may contain important information on the underlying biological process. In particular some cells display two distinct areas of triplet lifetime in the initial stage of the endocytosis, when all the transferrin is fully endocytosed (t = 5 min in Figure 5). The perinuclear recycling compartment appears to have two distinct areas: in the center of the compartment, the triplet lifetime corresponds to the lifetime we expect for the TMR-label ($\tau_{T,\,center} \approx 2.1\mu s$). However in some cells, the outer region of the perinuclear recycling compartment shows a distinctively different triplet lifetime of $\tau_{T,\,surrounding} \approx 3.3\mu s$. Compared to the background, this outer region appears much larger and more connected than the typical autofluorescence dots visible in Fig. 5 (f). Further on the intensity in this region is stronger when compared to the background ($I_{surrounding} \approx 75$, $I_{background} \approx 50$ and $I_{center} \approx 125$, where the average was calculated over an area of $\approx 4\mu m^2$). Further studies on the exact biological origin of these distinct areas have yet to be done.

In conclusion Triplet Lifetime Imaging proves to be a valuable and versatile tool for the assessment of internalization and recycling of proteins in single living cells. As we demonstrate in this study, it extends the analysis beyond the limitations of purely intensity based measurements and improves the sensitivity of these measurements. This method has the potential to become a simple and valuable tool for *in-situ* assessment of the recycling rate of cell membrane receptors or their ligands.

Acknowledgements

The authors would like to thank Prof. Florian Wurm and all other members of the LBTC/EPFL, in particular, Virginie Bachmann and Mattia Matasci, for their help and support with the cell work. We would like to recognize Iwan Märki and Dimitri Van De Ville for fruitful discussions.